2013 IEEE/RSJ International Conference on
Intelligent Robots and Systems (IROS)
November 3-7, 2013. Tokyo, Japan

A Disturbance Observer for the sigma.7 Haptic Device

Andreas Tobergte and Patrick Helmer

***Abstract*— This paper presents a disturbance observer for the sigma.7 haptic device. External torques on the haptic device links are observed to distinguish between intended user interaction and accidental collisions of the links. Collisions can be unintentional contact of the human operator, e.g. with his knee, other people accidentally getting in contact with the haptic device or objects falling on it. The observer is based on the dynamic model of the device and sensor measurements from the joint‘s position sensors and an integrated force/torque sensor. Is is implemented concurrently with a control algorithm that uses the force/torque sensor to effectively reduce the inertia and friction of the sigma.7. Furthermore, forces and torques applied on the grasping unit by the human operator are observed. Experiments are done with the sigma.7 customized for the German Aerospace Center (DLR) by Force Dimension.**

I. INTRODUCTION

The sigma.7 haptic devices are designed with respect to the requirements in minimally invasive robotic surgery (MIRS) and other medical applications. Specifications are derived form the MiroSurge system at DLR (German Aerospace Center) which is is a prototype for minimally invasive robotic surgery [4] [5]. The devices are designed by Force Dimension to be integrated into the MiroSurge operator console [11], as shown in Fig. 1. Dedicated left and right handed devices are integrated in the console in an ergonomic configuration. Each of the devices is fully actuated in seven degrees of freedom (DoF). The mechatronic structure of the sigma.7 haptic input device comprises three main components: translational base, rotational wrist extension and grasping unit. The translational base has a parallel kinematics structure of the ”delta” family [2] with three independent kinematic chains fixed to the device base and joint together at the translational base output. The rotational wrist extension is mounted on the translational base output and has a serial kinematics structure with an arrangement of three pivot joints having intersecting axes. This advantageous design leads to inherently decoupled kinematics and dynamics. Cartesian output forces are up to 20 N within the translational workspace, which is a sphere of about 120 mm diameter for each device. The rotational wrist of the device covers the whole workspace of the human hand and provides maximum torques of about 0.4 Nm. The grasping unit, attached to the rotational wrist, can display forces up to 8 N.

The sigma.7 developed for DLR also integrates an off-the-shelf 6 DoF force/torque sensor (Nano-17, ATI Inc., USA). In [11] a control algorithm based on the force/torque measurements was presented. The controller implements a scaling of the inertia and friction of the device to about one half. The impedance felt by the user is effectively reduced allowing more transparent force-feedback and also a more precise command of motions. In [12] a user study was done where the subjects were asked to track a virtual ball in 3 DoF with the sigma.7. The experiments show that the tracking error was reduced when the inertia and friction was reduced by means of control. The 2012 version of the sigma.7 for DLR also features improved encoder resolution and timing of the sensor electronics, which leads to better calculated derivatives.

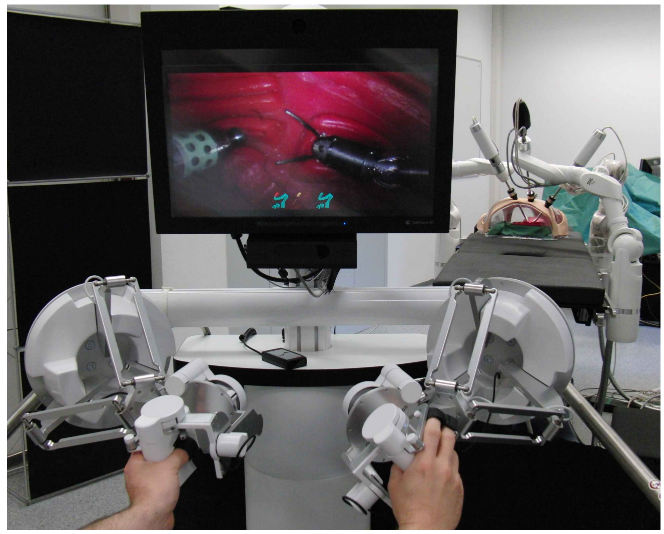

Fig. 1. Foreground: Operator console with bi-manual sigma.7 and auto-stereoscopic display; Background: Three MIRO arms attached to an operating table, two holding MICA instruments and one holding a stereo endoscope

The integrated force/torque sensor and improved encoder measurements also allows to implement model-based observers that are presented in this paper. The observed properties are:

- Disturbances on the link structure
- Interaction forces on the grasping unit

The disturbances on the link structure can be used to trigger an emergency clutch [10] that disconnects master from slave if a certain threshold is exceeded, i.e. the disturbance is interpreted as a collision.

Collision detection of haptic devices is not addressed in literature, as far as the authors are aware. It is generally assumed that the human operator’s hand holding the handle or grasping interface is the only force/torque input on the

Andreas Tobergte is with the Institute of Robotics and Mechatronics, DLR - German Aerospace Center, Wessling, Germany andreas.tobergte@dlr.de
Patrick Helmer is with Force Dimension, Nyon, Switzerland helmer@forcedimension.com

978-1-4673-6357-0/13/$31.00 ©2013 IEEE

device. However, in surgery such collisions can be safety critical and if an open console concept is preferred such as the MiroSurge console (Fig. 1) accidental contacts by the operation room staff can not be fully excluded. Also collisions of the human operator's knee and the sigma.7 delta structure are possible. However, collision detection and avoidance was addressed for robots. A collision observer based on an impulse formulation of the robot dynamics using the integrated torque sensors of the KUKA/DLR Light weight robot is presented in [3]. Collisions can be detected when the robot is initially in free motion.

In literature, if haptic devices are equipped with force/torque sensing, the sensor is usually considered to be the distal end of the device, which is in direct contact with the human operator's hand, e.g. [6], [1]. The interaction forces applied by the human operator are considered to be directly measured. The sigma.7 integrates the sensor in the structure with the grasping unit being attached to the sensor. As a consequence the user force is not directly measured. In this paper an observer for the interaction force is presented. This is mainly for evaluation purposes.

The paper starts with a description of the dynamic model in section II. A control algorithm, including a proof of passivity is presented in section III. The disturbance observer and interaction observer are presented in section IV, followed by the experiments in section V. The paper finishes with a conclusion VI.

II. Dynamic Model

The machatronic structure of the sigma.7 haptic input device comprises three main components: translational base, rotational wrist extension and grasping unit. The dynamics of the sigma.7 can be described by combining the translational base and the wrist into a 6 DoF actuated mechanism for motion in space. The grasping is considered to be a separate

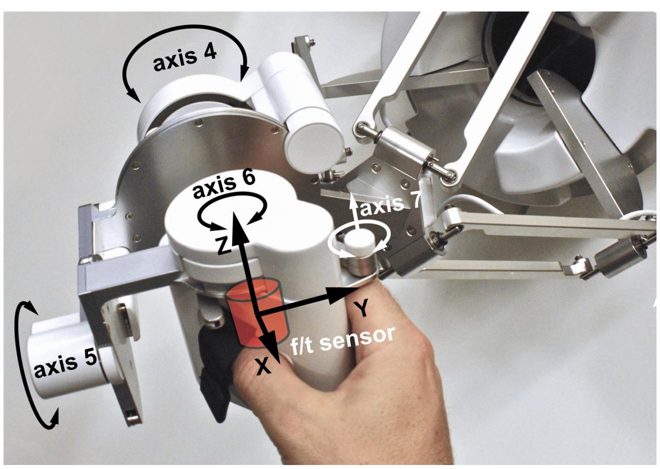

Fig. 2. Perpendicular axes of the rotational wrist with force-/torque sensor in the intersection point (HCP-frame) integrated in the mechanical structure; grasping unit (handle) attached to the sensor

functional DoF and the grasping unit is consequently treated as a passive handle attached to the force/torque sensor. The force/torque sensor, that connects the grasping unit and the 6 DoF mechanism, is located in the intersecting point of the three rotational axis. This point is also considered the reference frame for user interaction, the hand-center-point (HCP).

A. Equations of motion

The device dynamics is split up into two parts connected by the sensor: 1) the translational base and rotational wrist with motors and joints of axis 1 to 6, as well as the links; 2) the grasping unit (or handle). The controller presented here, refers to the first part with axes 1 to 6 that are required for motion in space. In Fig. 3 a model of the device is shown with all states/input/output variables in the 6 DoF joint space. The motor torque τ_m is actuating the motor inertia $\mathbf{B}$ that is assumed to be rigidly connected with the link inertia $\mathbf{M}_l$. Additional disturbances τ_{dist} and the sensor torque τ_s are affecting the motor and link motion.

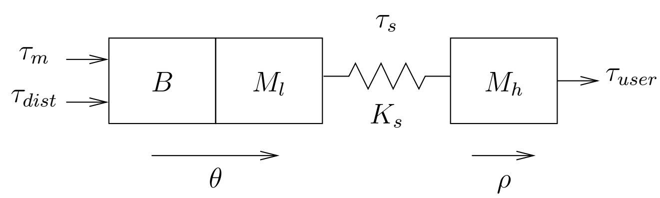

Fig. 3. Physical model of the sigma with the force/torque sensor as a spring; motor and link inertia are left; handle inertia is on the right side

The motor/link dynamics

$$(\mathbf{B}+\mathbf{M}_l(\theta))\ddot{\theta}+\mathbf{C}_l(\theta,\dot{\theta})\dot{\theta}+\mathbf{g}_l(\theta)+\tau_s+\tau_{dist}=\tau_m \quad (1)$$

is completed with the centripetal-/coriolis forces $\mathbf{C}_l(\theta,\dot{\theta})\dot{\theta}$ and gravity $\mathbf{g}_l(\theta)$, where $\theta \in \Re^6$ represents the motor side joint angles and $\dot{\theta}$) represent the corresponding velocities. The disturbances τ_{dist} acting on the motors and links are composed of internal and external disturbances. The internal disturbance is friction τ_{fric}, that exists primarily in the motors. External disturbances τ_{ext} are collisions of the link structure with objects or humans.

$$\tau_{dist}=\tau_{fric}+\tau_{ext} \quad (2)$$

The handle side angles in joint space are given with ρ in the dynamics of the handle:

$$\mathbf{M}_h(\rho_r,\gamma)\ddot{\rho}+\mathbf{g}_h(\rho_r,\gamma)=\tau_s+\tau_{user} \quad (3)$$

The user torque τ_{user} is an unmeasured input, whereas the sensor torque τ_s is modeled as an internal state. Inertia $\mathbf{M}_h(\rho_r,\gamma)$ and gravity $\mathbf{g}_h(\rho_r,\gamma)$ of the handle depend on the rotational axis ρ_r only, as well as the opening angle of the grasping γ. The sensor torque connects link and handle positions

$$\tau_s=\mathbf{K}_s(\theta-\rho) \quad (4)$$

with the sensor stiffness $\mathbf{K}_s$. Note, that the deformation $\theta-\rho$ is rather small and can be considered to be a negligible deformation because the sensor stiffness is very high. [1]

[1] translational stiffness $\geq 10^6 \frac{N}{m}$; www.ati-ia.com; February 2011

B. Static Decoupling

The kinematics of the sigma.7 device can be advantageously described by completely decoupling the translational workspace from the rotational one. The Jacobian $\mathbf{J}(\theta)=\frac{\delta \mathbf{x}}{\delta \theta}$ with Cartesian space $\mathbf{x} \in SE3$ and joint space $\theta \in \Re^6$, referring to axis 1 to 6, consists of two independent Jacobian matrices of dimension 3×3.

$$\mathbf{J}(\theta)=\begin{pmatrix} \mathbf{J}_t(\theta_t) & \mathbf{0} \\ \mathbf{0} & \mathbf{J}_r(\theta_r) \end{pmatrix} \tag{5}$$

The static decoupling of translations and rotations is a direct consequence of the kinematic decoupling, since the Cartesian forces and torques are linked with the joint torques by the transposed Jacobian.

C. Dynamic Decoupling

The dynamics of the sigma.7 is widely decoupled with the inertia matrix being nearly diagonal. However, there are some couplings because the wrist center of mass is not coincident with its center of rotation. This is barely noticeable to the operator under normal usage of the input device. The six dimensional link mass matrix takes into account all link masses and inertia, with exception of parallel bars inertia.

In the center of the workspace $\theta_0=[\theta_{t,0};\theta_{r,0}]$, the combined motor and link mass matrix is $[10^{-3}kgm^2]$:

$$\mathbf{B}+\mathbf{M}_l(\theta_0)=$$
$$\begin{pmatrix} 9.71 & -1.21 & -1.21 & 0.92 & 0.36 & -0.13 \\ -1.21 & 9.71 & -1.21 & -0.45 & -0.04 & 0.08 \\ -1.21 & -1.21 & 9.71 & -0.63 & -0.19 & -0.33 \\ 0.92 & -0.45 & -0.63 & 1.45 & -0.02 & 0.02 \\ 0.36 & -0.04 & -0.19 & -0.02 & 0.51 & 0.00 \\ -0.13 & 0.08 & -0.33 & 0.02 & 0.00 & 0.24 \end{pmatrix}$$

The corresponding Cartesian inertia

$$\mathbf{B}_C+\mathbf{M}_{l,C}(\theta)=\mathbf{J}(\theta)^{-T}(\mathbf{B}+\mathbf{M}_l(\theta))\mathbf{J}(\theta)^{-1} \tag{6}$$

is given with the Jacobian. The reflected Cartesian inertia of the translational base with motors and links

$$\mathbf{B}_{t,C}(\theta_{t,0})+\mathbf{M}_{l,t,C}(\theta_{t,0})=\begin{pmatrix} 1.84 & 0 & 0 \\ 0 & 1.50 & 0 \\ 0 & 0 & 1.50 \end{pmatrix}[kg]$$

is fully decoupled in the center of the workspace. The translational Cartesian inertia of the grasping unit $\mathbf{M}_{h,r,C}$ is $0.259kg$ on the diagonal elements.

III. Control

In this section a controller using the force-/torque sensor of the sigma.7 is presented. The torque controller in joint space can be interpreted as a scaling of the device dynamics. Even though the sigma.7 already shows low inertia and friction without torque control, the strong motors for all seven DoF and the rigidly designed mechanics have a certain influence. In minimally invasive robotic surgery the device usage goes beyond hard contact discrimination to perception of small stiffness variations of soft tissue. Especially for sensitive palpation tasks, e.g. for detecting and localizing a tumor, lower inertia and friction are beneficial to increase the transparency.

A state feedback controller can be selected,

$$\tau_m=r\cdot\mathbf{u}+(1-r)\tau_s+\mathbf{g}_l(\theta) \tag{7}$$

where r is a positive gain. The vector $\mathbf{u}$ represents a new torque input. The control uses the measured joint angles and the measured wrench of the force/torque sensor transformed into joint space with the Jacobian. Inserting (7) into (1) leads to the closed loop dynamics of the motor/link system. Inertia, friction, centripetal-/coriolis forces and disturbance torques are reduced proportional to r^{-1}.

$$r^{-1}(\mathbf{B}+\mathbf{M}_l(\theta))\ddot{\theta}+r^{-1}\mathbf{C}_l(\theta,\dot{\theta})\dot{\theta}+\tau_s+r^{-1}\tau_{dist}=\mathbf{u} \tag{8}$$

Gravity of the links can be fully compensated. Adding gravity compensation of the handle

$$\mathbf{u}=-\mathbf{u}_{app}+\mathbf{g}_h(\bar{\rho}) \tag{9}$$

gives the application input $\mathbf{u}_{app}$. Gravity compensation is based on a motor sided estimation of the handle sided angles $\bar{\rho}$, which is statically equivalent to ρ [7]. However, in the given case of a very stiff sensor, one can simply use $\bar{\rho}\approx\theta$.

The closed loop system is passive, which is desirable to increase the robustness in contact and to allow the connection with different applications, as shown in Fig. 4. The system is a degenerative connection of passive subsystems [9].

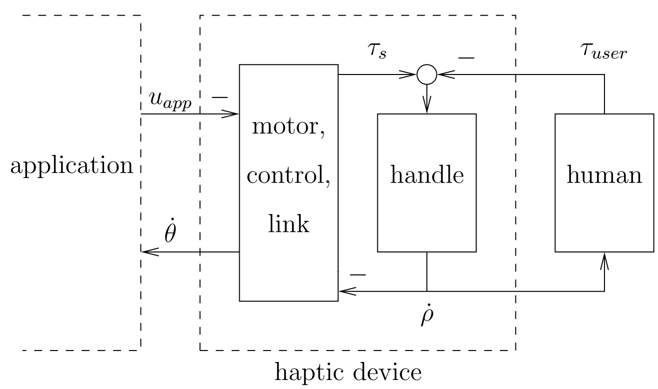

Fig. 4. System with haptic device, human operator and application as interconnection of passive subsystems

The human operator and the handle are passive. The application needs to be passive with an impedance port of ingoing velocities and outgoing forces (torques). What remains to be shown, is that the subsystem with motors, control and links is passive. In general, it can potentially be active due to the actuators.

A system ($\mathbf{u}\rightarrow\mathbf{y}$) is passive, if there exists a continuous storage function S [8], which is bounded from below and for which the derivative satisfies the inequality $\dot{S}\leq\mathbf{y}^T\mathbf{u}$.

Inserting (9) into (8) gives the dynamics of the motor/control/link subsystem,

$$\frac{1}{r}(\mathbf{B}+\mathbf{M}_l(\theta))\ddot{\theta}+\frac{1}{r}\mathbf{C}_l(\theta,\dot{\theta})\dot{\theta}+\mathbf{u}_{app}+\tau_s+\frac{1}{r}\tau_{dist}=\mathbf{g}_h(\bar{\rho}) \tag{10}$$

in which the inertial torques, as well as the disturbance torques, including friction and external torques are scaled. The storage function as a mapping of $(\dot{\rho} \rightarrow \tau_s)$ is given by

$$S = \frac{1}{2r}\dot{\theta}^T(\mathbf{B}+\mathbf{M}_l(\theta))\dot{\theta} + \frac{1}{2}(\theta-\rho)^T\mathbf{K}_s(\theta-\rho) - V_{g_h}(\bar{\rho}) \tag{11}$$

with the kinetic energy of the scaled inertia and the potential energy of the spring (sensor) and the gravity. The energy of the inertia and the spring are greater or equal zero and gravitational energy is lower bounded. It follows directly that S is lower bounded. Furthermore, with gravity compensation based on $\mathbf{g}_h(\bar{\rho})$ the device is in a static equilibrium in any pose. The derivative

$$\dot{S} = -r^{-1}\dot{\theta}^T\tau_{fric} - r^{-1}\dot{\theta}^T\tau_{ext} - \dot{\theta}^T\mathbf{u}_{app} - \dot{\rho}^T\tau_s \tag{12}$$

describes the power balance by using (2). The first term is the friction power, which is passive by definition. The second term is the power of the external disturbance. The last two terms describe the ports of the subsystem, as shown in Fig. 4. It follows that the motor/control/link subsystem is passive, if the connected subsystems are passive. Connected subsystems that are active will not stimulate activity in the motor/control/link subsystem. It will not generate energy but only transport the induced energy, e.g. from the collision to the handle.

IV. Observers

A disturbance observer for estimation of external torques on the links and detection of collisions can be defined based on the dynamic model and the force/torque sensor, as well as the encoder measurements of the motors.

The observer is defined by solving (1) for the disturbance torque

$$\hat{\tau}_{dist} = \tau_m - \tau_s - (\mathbf{B}+\mathbf{M}_l(\theta))\ddot{\theta} - \mathbf{g}_l(\theta) \tag{13}$$

where the corioli- and centripetal torques can be neglected. An additional low-pass filter is applied to deal with the noise of the acceleration, which is derived from position measurements. The norm of the disturbance torque,

$$||\hat{\tau}_{dist}|| = (\hat{\tau}^2_{dist,1} + ... + \hat{\tau}^2_{dist,6})^{1/2} \tag{14}$$

defined as the Euclidean norm of a vector, is used as an indicator for collisions on the links or moving structural elements of the sigma.7. Evaluating the norm over all joints leads to an emphasis of the translational base, which has higher inertia. It also amplifies peaks, due to using the square of each joint, and suppresses low magnitude friction effects.

The user torque can be observed with an interaction observer

$$\hat{\tau}_{user} = \mathbf{M}_h(\rho_r,\gamma)\ddot{\rho} + \mathbf{g}_h(\rho_r,\gamma) - \tau_s \tag{15}$$

that solves (3) for the user torque, where $\rho = \theta$. Similarly, to the disturbance observer an additional low-pass filter is applied.

V. Experiments

The disturbance observer and the interaction observer, where implemented and tested with the sigma.7, DLR version of 2012. All experiments were done in combination with the torque controller, presented in section III. The dynamic scaling factor was set to $r^{-1} = 0.5$. The experiments are benchmark tests, where either the grasping unit or the links have contact, but not simultaneously as with a real collision during an application. In general, contacts on the links are easier to detect, when the human operator holds the grasping unit in his hand and applies some resistance, either intentionally or by the natural impedance of the human arm.[2]

A. Ball hits haptic device

A first experiment was done with a sponge ball falling on the device. The ball was loaded with a small piece ot metal inside, so the total weight is $0.02kg$. The Ball falls from a dropping height of approximately $0.02m$ on the grasping unit and on the link structure, as indicated in Fig. 5. The impact on the handle is equivalent to a user input τ_{user}, whereas the impact on the link in an external input τ_{ext}. Due to the decoupled characteristics of the sigma.7, the impact in gravitational direction also generates a motion of the device downwards in z-direction, while the other DoF are relatively unaffected.

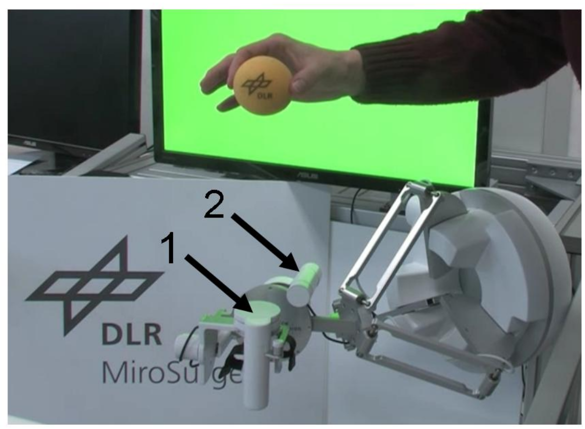

Fig. 5. Ball is dropped on the grasping unit (1) and on the link structure (2), the monitor indicates collisions

The norm of the disturbance torque $||\hat{\tau}_{dist}||$, as defined in (14) is shown in Fig. 6. The torque is about 2.5 times higher when the Ball falls on the structure and can be clearly identified as a peak related to the impact.

In Fig. 7 the corresponding forces, velocities, positions in z-axis are shown. The ball impact results in a sensor force, if the ball falls on the handle (top, left, green) and a disturbance force if it falls on the structure (top, right, black). The forces are the z-components of the Cartesian wrench of τ_s and $\hat{\tau}_{dist}$, respectively. For easier comparison the sensor force

[2]Please, refer to the video attached.

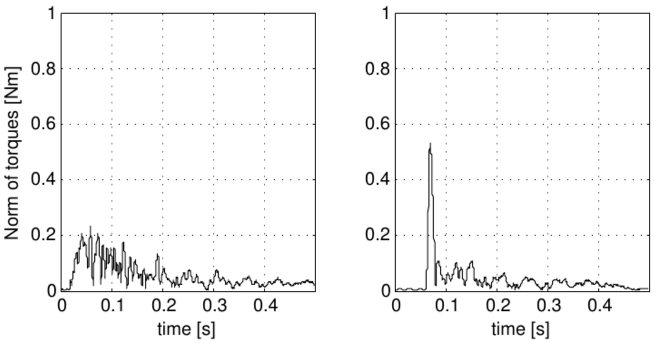

Fig. 6. Norm of disturbance torques with dropping ball; Left: Ball falls on grasping unit; Right: Ball falls on link structure

in plotted without the gravitational force. The velocity and the position displacement caused by the impact are roughly twice as high if the ball falls on the grasping unit. This is to be expected because the contact on the handle effects the dynamics scaled by the torque controller, whereas the impact on the structure effects the unscaled dynamics.

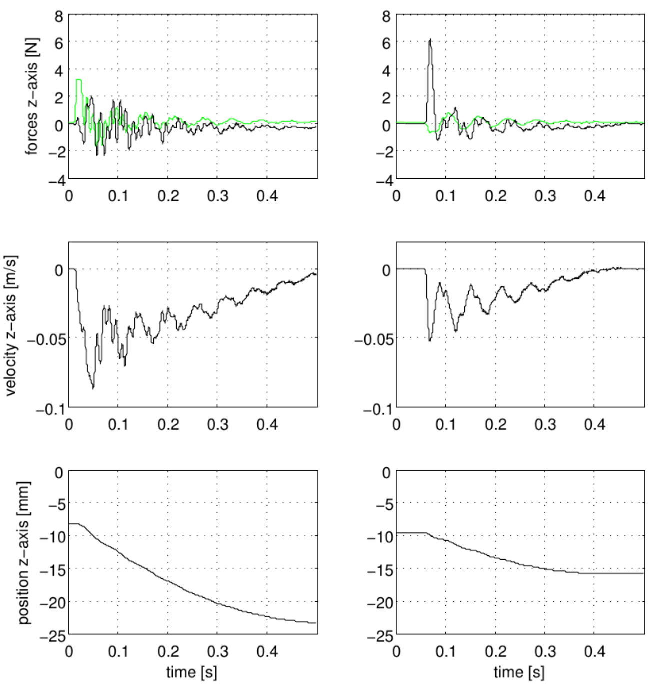

Fig. 7. Ball impact in z-axis; Top: sensor force (green) and disturbance force (black); Middle: velocity; Bottom: position; Left: Ball falls on grasping unit; Right: Ball falls on link structure

B. Manual motion

Another experiment was done with the haptic device being manually moved in the horizontal plane on the y-axis (left-right). Fig. 8 shows the norm of the disturbance torques, with the hand on the grasping unit (left) and on the structure (right). The norm is about three times higher when touched on the structure, while the velocity of the sinusoidal motion in similar, as it can be seen in Fig. 9.

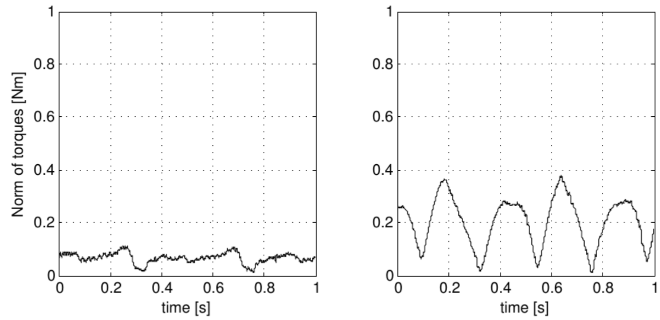

Fig. 8. Norm of disturbance torques with manual motion; Left: Touch on grasping unit; Right: Touch on link structure

It can also be seen that the disturbance force in the y-axis, when touched on the handle (left, top, black) is in phase with the velocity (left, middle). This is an indication that the property observed is friction. In case that the device is moved by touching the structure the observed external force (right, bottom, black) is zero, where the sensor force (right, bottom, green) shows the inertial force of the grasping unit.

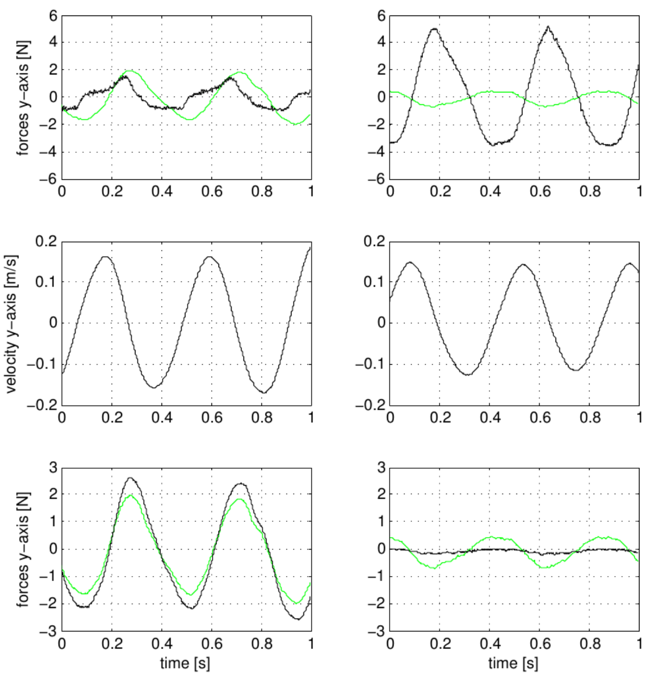

Fig. 9. Manual motion in y-axis; Top: sensor force (green) and disturbance force (black); Middle: velocity; Bottom: sensor force (green) and user force (black); Left: Touch on grasping unit; Right: Touch on link structure

C. Contact with virtual wall

A third experiment was done hitting against a virtual wall in the y-axis. As above, Fig. 10 shows the norm of the disturbance torques, with the hand on the grasping unit (left) and on the structure (right). The disturbance norm is about four times higher, when the structure is touched, while the velocity profiles are similar, as shown in Fig. 11.

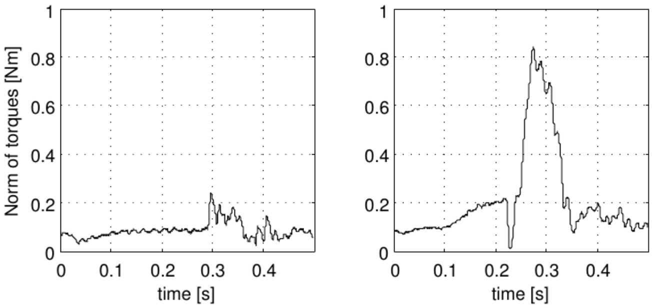

Fig. 10. Norm of disturbance torques when hitting a virtual wall; Left: Touch on grasping unit; Right: Touch on link structure

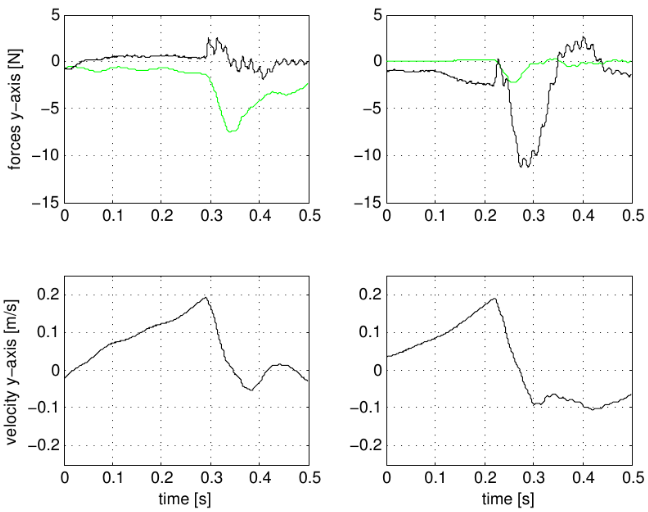

Fig. 11. Hitting a virtual wall in y-axis; Top: sensor force (green) and disturbance force (black); Bottom: velocity; Left: Touch on grasping unit; Right: Touch on link structure

D. Summary

The experiments compare benchmark tests, that evaluate three situations, at first with contact on the grasping unit and at second with contact on the link structure. In all cases the norm of the disturbance torques with contact on the structure is a multiple of the one with contact on the grasping unit. One can also see that the disturbance observation gets less precise when impacts like a colliding ball or high motor torques of a virtual wall are causing vibrations in the whole apparatus including the mounting of the device. In the presented experiments a threshold of $\tau_{limit} = 0.25Nm$ clearly separates collisions on the structure from inputs on the grasping unit. In real applications, where the human operator always holds the grasping unit with a certain impedance the threshold can be increased, because collisions generate higher torque peaks.

VI. Conclusion

In this paper a disturbance observer and an interaction observer for the sigma.7 haptic device was presented. The observers run concurrently with a torque controller that effectively reduces the inertia of the device and disturbances, like friction and external contacts on the links. Apart from reducing the impacts of collisions by humans or objects directly with the controller, the impacts can also be detected with the disturbance observer. The interaction forces/torques applied by the human operator on the grasping unit are also observed, which can be used for evaluation. Experiments with benchmark scenarios were presented that show the validity of the approach. All experiments were done with the sigma.7 DLR version 2012 and the presented observers will be integrated into the DLR MiroSurge system.

VII. Acknowledgment

The research leading to these results has received funding from the European Union Seventh Framework Programme (FP7/2007- 2013) under grant agreement n248960.

References

[1] Jorge Juan Gil and Emilio Sanchez. Control algorithms for haptic interaction and modifying the dynamical behaviour of the interface. In *Proceedings of Enactive, Genova, Italy*, 2005.

[2] S. Grange, F. Conti, P. Rouiller, P. Helmer, and C. Baur. The Delta Haptic Device. In *Mecatronics 2001*, 2001.

[3] S. Haddadin, A. Albu-Schaffer, A. De Luca, and G. Hirzinger. Collision detection and reaction: A contribution to safe physical human-robot interaction. In *Intelligent Robots and Systems, 2008. IROS 2008. IEEE/RSJ International Conference on*, pages 3356–3363, Sept.

[4] U. Hagn, R. Konietschke, A. Tobergte, M. Nickl, S. Jörg, B. Kuebler, G. Passig, M. Gröger, F. Fröhlich, U. Seibold, L. Le-Tien, A. Albu-Schäffer, A. Nothelfer, F. Hacker, M. Grebenstein, and G. Hirzinger. DLR MiroSurge - a versatile system for research in endoscopic telesurgery. *International Journal of Computer Assisted Radiology and Surgery*, 2009.

[5] U. Hagn, T. Ortmaier, R. Konietschke, B. Kuebler, U. Seibold, A. Tobergte, M. Nickl, S. Jörg, and G. Hirzinger. Telemanipulator for remote minimally invasive surgery. *IEEE Robotics & Automation Magazine*, 15(4):28–38, December 2008. DOI: 10.1109/MRA.2008.929925.

[6] D. Lawrence. Stability and transparency in bilateral teleoperation. In *IEEE transactions on robotics and automation*, 1993.

[7] Ch. Ott, A. Albu-Schäffer, A. Kugi, S. Stramigioli, and G. Hirzinger. A passivity based Cartesian impedance controller – part I: Torque feedback and gravity compensation. In *Proceedings of the IEEE International Conference on Robotics and Automation (ICRA)*, New Orleans, USA, 2004.

[8] A. J. Van der Schaft. *L2-Gain and Passivity Techniques in Nonlinear Control*. Springer-Verlag New York, Inc., Secaucus, NJ, USA, 1st edition, 1996.

[9] Jean-Jacques Slotine and Weiping Li. *Applied Nonlinear Control*. Prentice Hall, October 1990.

[10] Andreas Tobergte and Alin Albu-Schäffer. Direct force reflecting teleoperation with a flexible joint robot. In *Proceedings of the IEEE International Conference on Robotics and Automation (ICRA)*, Saint Paul, Minnesota, USA, 2012.

[11] Andreas Tobergte, Patrick Helmer, Ulrich Hagn, Patrice Rouiller, Sophie Thielmann, Sébastien Grange, Alin Albu-Schäffer, François Conti, and Gerd Hirzinger. The sigma.7 haptic interface for mirosurge: A new bi-manual surgical console. In *International Conference on Intelligent Robots and Systems (IROS)*, San Francisco, USA, 2011.

[12] B. Weber, A. Hellings, A. Tobergte, and M. Lohmann. Human performance and workload evaluation of input modalities for telesurgery. In *Proceedings of the German Society of Ergonomics (GfA)*, pages 409–412, 2013.